ELSEVIER

www.elsevier.nl/locate/jorganchem

Journal of Organometallic Chemistry 590 (1999) 138–148

Journal of Organometallic Chemistry

Rhenium(I) methoxo carbonyl complexes containing tetraphosphine or triphosphine ligands; facile separation and X-ray crystallographic studies of *d*/*l*- and *meso*-[{Re_2(μ-OMe)$_2$-(CO)$_6$}$_2$(μ,μ′-1,1,4,7,10,10-hexaphenyl-1,4,7,10-tetra-phosphadecane)]

Chenghua Jiang [a], Yuh-Sheng Wen [b], Ling-Kang Liu [b], T.S. Andy Hor [a,1], Yaw Kai Yan [c,*]

[a] *Department of Chemistry, Faculty of Science, National University of Singapore, Kent Ridge, Singapore 119260, Singapore*
[b] *Institute of Chemistry, Academia Sinica, Taipei 11529, Taiwan*
[c] *Division of Chemistry, National Institute of Education, Nanyang Technological University, 469 Bukit Timah Road, Singapore 259756, Singapore*

Received 22 June 1999; accepted 26 July 1999

Abstract

Reaction of the activated mixture of $Re_2(CO)_{10}$, Me_3NO and MeOH with a 1:1 mixture of *rac* (*d*/*l*)- and *meso*-1,1,4,7,10,10-hexaphenyl-1,4,7,10-tetraphosphadecane (hptpd) yields a mixture of (*d*/*l*)- and *meso*-[{Re_2(μ-OMe)$_2$(CO)$_6$}$_2$(μ,μ′-hptpd)] **1**. The diastereomers can be easily separated by selective dissolution of *d*/*l*-**1** in benzene, and give clearly distinguishable ^{1}H- and ^{31}P-NMR spectra. The fluxional behavior of *d*/*l*-**1** in solution has been studied by variable-temperature ^{1}H- and ^{31}P-{^{1}H}-NMR spectroscopy. The crystal structures of both *d*/*l*- and *meso*-**1** have been determined. Both molecules consist of two {Re_2(μ-OMe)$_2$(CO)$_6$} moieties which are bridged by the two P–CH_2–CH_2–P moieties of the hptpd ligand. Whilst the molecules of *meso*-**1** possess crystallographic *i*-symmetry, those of *d*/*l*-**1** do not have any crystallographic symmetry. These diastereomers therefore give clearly distinguishable Raman spectra in the solid state. Reaction of tris[2-(diphenylphosphino)ethyl]phosphine (tdppep) with the activated mixture affords the complex [{Re_2(μ-OMe)$_2$(CO)$_6$}(μ,η^2-tdppep)] **2**, and the analogous reaction involving bis[2-diphenylphospinoethyl)phenylphosphine (triphos) gives [{Re_2(μ-OMe)$_2$(CO)$_6$}(μ,μ′,η^3-triphos){Re_2(CO)$_9$}] **3** and [{Re_2(μ-OMe)$_2$(CO)$_6$}(μ,η^2-triphos)] **4**.

Keywords: Rhenium carbonyl; Amine *N*-oxide; Carbonyl–methoxo complex; Triphosphine; Tetraphosphine; Multinuclear aggregates

1. Introduction

Low-valent transition metal alkoxo complexes continue to be the focus of much research [1], being postulated as intermediates in many important metal-catalyzed organic transformations [2]. The synthesis, characterization and reactions of rhenium(I) carbonyl alkoxo complexes is the subject of our current interest [3]. Our studies indicated that the reaction of $Re_2(CO)_{10}$ with Me_3NO and MeOH results in a complex mixture of mono-, di- and trinuclear rhenium(I) methoxo species, as well as the Re–Re bonded species [$Re_2(CO)_9$(solvent)] [3b]. The mono- and dinuclear methoxo species have been trapped by coordination with diphosphines (PP) [3b–e], and it appears that the diphosphines are most adept at trapping and stabilizing the {Re_2(μ-OMe)$_2$} moiety, since [Re_2(μ-OMe)$_2$(μ-PP)(CO)$_6$] complexes are invariably the major phosphine-coordinated rhenium methoxo species formed in the reaction of diphosphines with the activated mixture of $Re_2(CO)_{10}$, Me_3NO and MeOH [3c–e]. The yield of the diphosphine-coordinated dirhenium methoxo complexes [Re_2(μ-OMe)$_2$(μ-PP)(CO)$_6$] decreases, however, with increasing length of the hydrocarbon chain linking the phosphino groups [3c].

We have now extended the above studies to include the triphosphines bis[2-diphenylphosphinoethyl)phenylphosphine (triphos) and 1,1,1-tris(diphenylphosphi-

* Corresponding author. Fax: +65-469-8952.
E-mail address: ykyan@nie.edu.sg (Y.K. Yan)
[1] Also corresponding author.

0022-328X/99/$ - see front matter
PII: S0022-328X(99)00442-8

nomethyl)ethane (tdppme), and the tetraphosphines 1,1,4,7,10,10-hexaphenyl-1,4,7,10-tetraphosphadecane (hptpd) and tris[2-(diphenylphosphino)ethyl]phosphine (tdppep). These phosphines are versatile multidentate ligands for transition metals in a variety of oxidation states, and their complexes have been the subject of studies of catalysis, structure–bonding relationships and spectroscopy [4–6]. The linear tetraphosphine hptpd is especially interesting since it can exist in three stereoisomeric forms (*d*, *l* and *meso*) [6] (Scheme 1). It is hoped that these multifunctional phosphines would be able to scavenge for and trap novel rhenium methoxo intermediates in the activated mixture, or facilitate the formation of novel multinuclear aggregates. It is also noteworthy that, amongst the numerous transition metal polyphosphine complexes reported, there are only a few polyphosphine complexes of rhenium [5a,7].

In this paper, we report the formation of the complexes (*d*/*l*)- and *meso*-[{Re_2(μ-OMe)$_2$(CO)$_6$}$_2$-(μ,μ′-hptpd)] **1**, [{Re_2(μ-OMe)$_2$(CO)$_6$}(μ,η^2-tdppep)] **2**, [{Re_2(μ-OMe)$_2$(CO)$_6$}(μ,μ′,η^3-triphos){Re_2(CO)$_9$}] **3** and [{Re_2(μ-OMe)$_2$(CO)$_6$}(μ,η^2-triphos)] **4** in the reactions of the respective polyphosphines with mixtures of $Re_2(CO)_{10}$, Me_3NO and MeOH (Scheme 2). We also report the crystal structures of both *d*/*l*- and *meso*-**1**, and the study of the fluxional behavior of *d*/*l*-**1** by variable-temperature ^{1}H- and ^{31}P-{^{1}H}-NMR spectroscopy. The solid-state laser Raman spectra of *d*/*l*- and *meso*-**1** in the CO-stretching region are also reported.

2. Results and discussion

2.1. Reaction of 1,1,4,7,10,10-hexaphenyl-1,4,7,10-tetraphosphadecane (hptpd) with $Re_2(CO)_{10}$, Me_3NO and MeOH

2.1.1. Formation of *d*/*l*- and *meso*-[{Re_2(μ-OMe)$_2$(CO)$_6$}$_2$(μ,μ′-hptpd)] **1**

The commercial hptpd used in this work is a roughly 1:1 mixture of *meso*- and *rac*-diastereomers, as shown by ^{31}P-{^{1}H}-NMR spectroscopy. This isomeric mixture was used directly for the reaction without pre-separation as described by Brown and Canning [8].

Reaction of hptpd with the mixture of $Re_2(CO)_{10}$, Me_3NO and MeOH gives the complexes *d*/*l*- and *meso*-[{Re_2(μ-OMe)$_2$(CO)$_6$}$_2$(μ,μ′-hptpd)] **1**, with a total yield of 18% (based on Re) and a *meso*:(*d*/*l*) ratio of ca. 3:2. We were also able to synthesize **1** from the controlled acidolysis [3a] of [Re_2(μ-OMe)$_3$(CO)$_6$]$^-$ in the presence of hptpd, with an improved total yield of 41% and a *meso*:(*d*/*l*) ratio of ca. 3:5. The different isomeric ratios obtained by the different synthetic routes can be attributed to the difference in reaction mechanisms [3a, b]. Interestingly, although *d*/*l*- and *meso*-**1** have very similar R_f values and hence cannot be effectively separated by TLC, they exhibit a great difference in solubility. While *meso*-**1** is almost insoluble in benzene, *d*/*l*-**1**

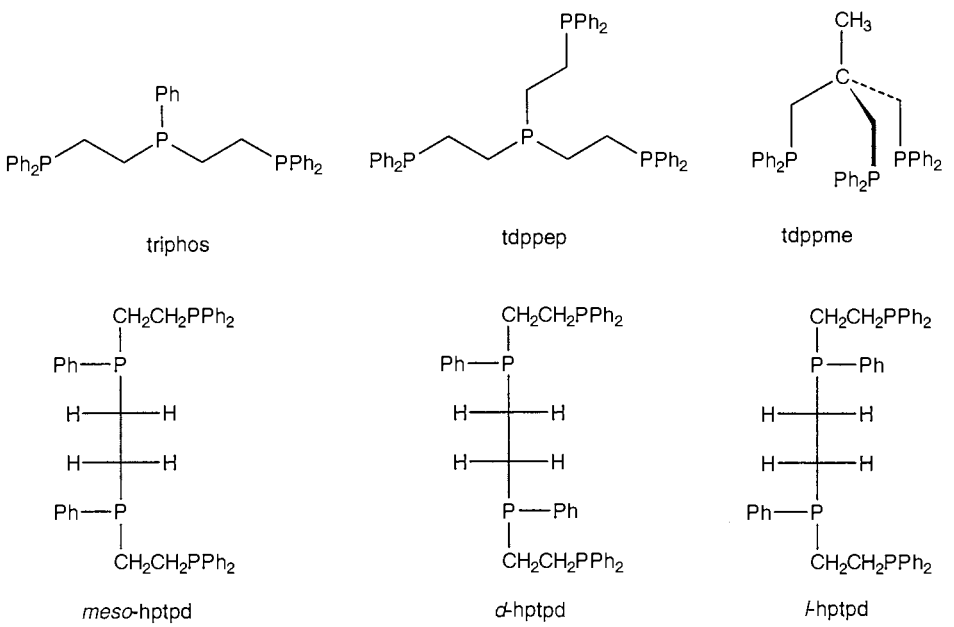

Scheme 1.

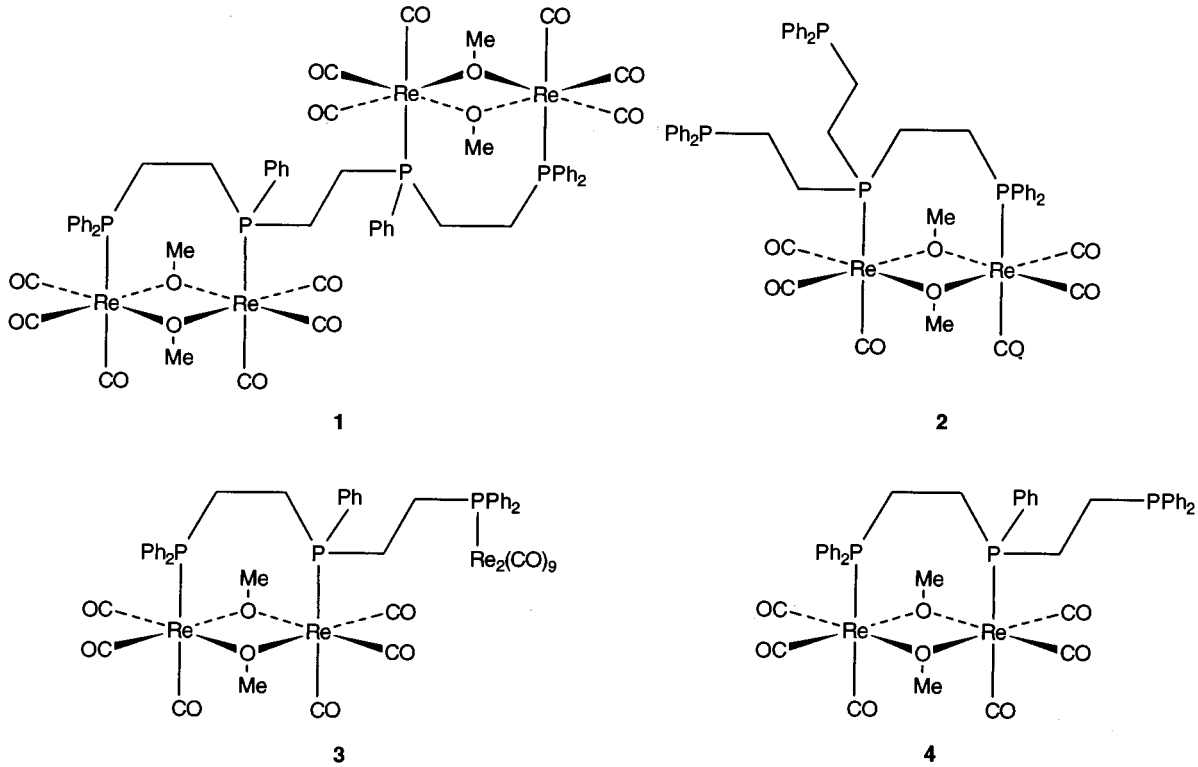

Scheme 2.

is readily soluble. This unusual property allows the two diastereomers of **1** to be easily separated by benzene extraction, hence obviating the need for pre-separation of the diastereomers of the hptpd ligand, as described in many reports of hptpd complexes [6]. The solubility difference between *meso*- and *d*/*l*-**1** is also consistent with that between *meso*- and *rac*-hptpd–*rac*-hptpd is more soluble than *meso*-hptpd in tetrahydrofuran [9].

2.1.2. Crystal structures of meso- and d/l-[{Re$_2$(μ-OMe)$_2$(CO)$_6$}$_2$(μ,μ′-hptpd)] 1

The molecules of both *meso*-**1** (Fig. 1) and *d*/*l*-**1** (Fig. 2) consist of two {$Re_2(\mu\text{-}OMe)_2(CO)_6$} moieties which are bridged by the two P–CH_2–CH_2–P moieties of the hptpd ligand. Thus, the complexes can be thought of as 'dimers' of the dppe complex [$Re_2(\mu\text{-}OMe)_2(\mu\text{-}dppe)(CO)_6$] [3c]. This clearly illustrates the ability of short-chain diphosphines to stabilize the {$Re_2(\mu\text{-}OMe)_2$} moiety.

Although the molecule of *meso*-**1** possesses crystallographic *i*-symmetry, so that only one-half of the molecule (consisting of one {$Re_2(\mu\text{-}OMe)_2(CO)_6$} fragment and half of the hptpd ligand) is unique, the asymmetrical substitution of P(1) and P(1a) results in the two μ-OMe groups of each {$Re_2(\mu\text{-}OMe)_2(CO)_6$} fragment being non-equivalent. Consequently, the solution ^{1}H-NMR spectrum of *meso*-**1** shows two separate peaks for the μ-OMe groups.

The Re(1)···Re(2) distance of 3.3966(9) Å in *meso*-**1** is comparable to those in [$Re_2(\mu\text{-}OMe)_2(\mu\text{-}dppf)(CO)_6$] [3.4042(6) Å] [3e] and [$Re_2(\mu\text{-}OMe)_2(\mu\text{-}dppm)(CO)_6$] [3.3917(7) Å] [3c]. However, the O–Re–O angle [average 73.1(3)°] in *meso*-**1** lies between those in [$Re_2(\mu\text{-}OMe)_2(\mu\text{-}dppf)(CO)_6$] [average 71.3(2)°] [3e] and [$Re_2(\mu\text{-}OMe)_2(\mu\text{-}dppm)(CO)_6$] [average 74.8(3)°] [3c]. These features of *meso*-**1** should be similar to those of [$Re_2(\mu\text{-}OMe)_2(\mu\text{-}dppe)(CO)_6$], which has not been structurally characterized.

The crystals of *d*/*l*-**1** (small elongated plates) diffracted rather weakly and gave diffraction data with a rather high R_{int} value (0.061 based on F^2). Consequently, the structural parameters determined have relatively high estimated S.D. Specifics of the bonding within the molecule are therefore not discussed; these are expected to be similar to those observed in *meso*-**1**. The essential features of the structure, however, have been established and hence an overall analysis of the gross features of the molecule is still considered valid.

In contrast to the structure of *meso*-**1**, the molecule of *d*/*l*-**1** has a distorted C_2 symmetry, resulting in all the phosphorus atoms and all the methoxo groups being non-equivalent. As in the *meso* isomer, however, the P–Re bonds in the different {$Re_2(\mu\text{-}OMe)_2(PP)$} fragments of *d*/*l*-**1** point in approximately opposite directions, probably to minimize steric repulsion between the two {$Re_2(\mu\text{-}OMe)_2(PP)$} fragments. The stereochemical

configurations at P(2) and P(3) and the requirement for the *trans* disposition of the two $\{Re_2(\mu\text{-}OMe)_2(PP)\}$ fragments force the backbone of the hptpd ligand in *d*/*l*-**1** into a U-shape, as shown in Fig. 2. This is in contrast to the molecule of *meso*-**1**, which adopts a linear configuration.

2.1.3. Variable-temperature ^1H- and ^{31}P-$\{^1H\}$-NMR spectra of *d*/*l*-**1**

The ^1H- and ^{31}P-$\{^1H\}$-NMR spectra of *meso*-**1** at ambient temperature show two ^1H peaks due to the methoxo ligands and two ^{31}P peaks, respectively. This is consistent with the crystal structure of *meso*-**1**. The room-temperature ^1H- and ^{31}P-$\{^1H\}$-NMR spectra of *d*/*l*-**1** also show two ^1H resonances for the methoxo ligands and two ^{31}P signals. This is, however, inconsistent with the crystal structure of *d*/*l*-**1**, and warrants a study of the variable-temperature ^1H- and ^{31}P-$\{^1H\}$-NMR spectra of the complex.

At 300 K the ^{31}P-$\{^1H\}$-NMR spectrum of *d*/*l*-**1** (Fig. 3) consists of two sharp singlets at 16.7 and 7.9 ppm, which are assigned to the terminal and internal phosphorus atoms, respectively, of the hptpd ligand. At 240 K, the peak at 7.9 ppm broadens and moves slightly upfield, eventually splitting into two peaks at 220 K. The peak at 16.7 ppm is however only slightly broadened at 220 K. At 200 K, the signals due to the internal phosphorus atoms become sharp and clear at 13.8 and -0.9 ppm, and the peak at 16.7 ppm is split into two sharp signals at 17.0 and 16.1 ppm. Thus, at 200 K there are four ^{31}P signals corresponding to the four non-equivalent phosphorus atoms in the crystal structure of *d*/*l*-**1**. At 190 K, the lowest temperature achievable for CD_2Cl_2, the two peaks at 13.8 and -0.9 ppm further split into doublets. This is attributed to the coupling between the two internal phosphorus atoms ($^3J_{P-P}$ ca. 17 Hz).

The two ^1H peaks of the μ-OMe groups at 300 K (4.35 and 4.17 ppm) are also split into four at 190 K, although these four peaks are still very broad (Fig. 4). The peak at 4.35 ppm broadens more quickly as temperature is lowered, and is split into two broad signals 4.54 and 4.08 ppm) at 200 K. The 4.17 ppm signal at 300 K, on the other hand, is only barely resolved into two peaks (4.18 and 4.16 ppm) at 190 K. From the structure of *d*/*l*-**1** (Fig. 2), it is apparent that two of the methoxo ligands [C(2) and C(3)] point inwards and the other two [C(1) and C(4)] point outwards. The signals at 4.54 and 4.08 ppm are assigned to the internal methoxo protons, which are expected to have a larger difference in chemical shifts due to the larger difference in their chemical environments.

The fluxional motion of the molecule most probably results in the exchange of chemical environments between the two internal methoxo groups and that between the two external methoxo groups, in terms of their spatial relationships with the phenyl rings. The same process probably causes the exchange of environments between the internal phosphorus atoms and that between the terminal phosphorus atoms, since the temperature-dependent behaviors of the ^{31}P and methoxo proton signals are very similar.

An exchange mechanism that is consistent with the above observations involves the twisting of the two terminal CH_2–CH_2 axes in the hptpd backbone. It is apparent from Fig. 2 that one of the terminal $\{PCH_2CH_2P\}$ segments [P(1)–P(2)] adopts a *δ gauche* conformation, while the other [P(3)–P(4)] adopts a *λ*

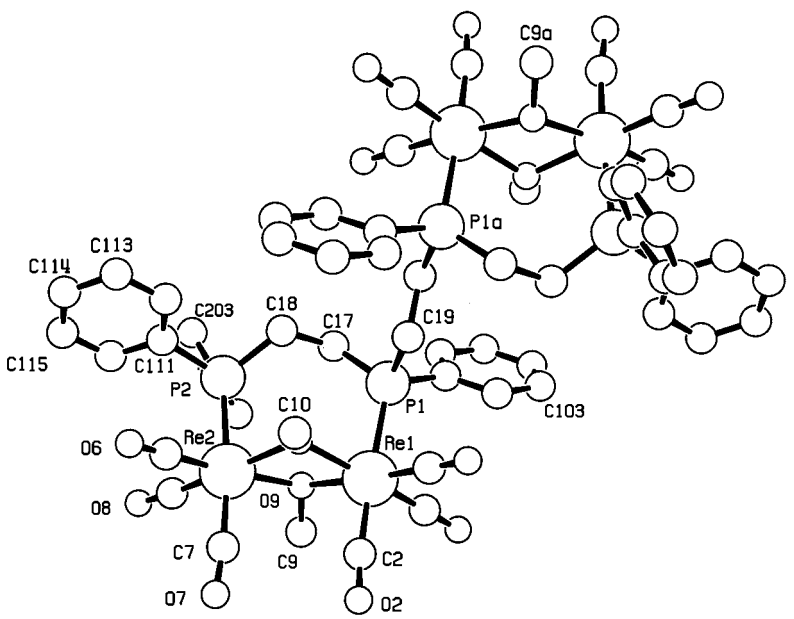

Fig. 1. Crystal structure of *meso*-[$\{Re_2(\mu\text{-}OMe)_2(CO)_6\}_2(\mu,\mu'$-hptpd)] **1** (hydrogen atoms omitted for clarity).

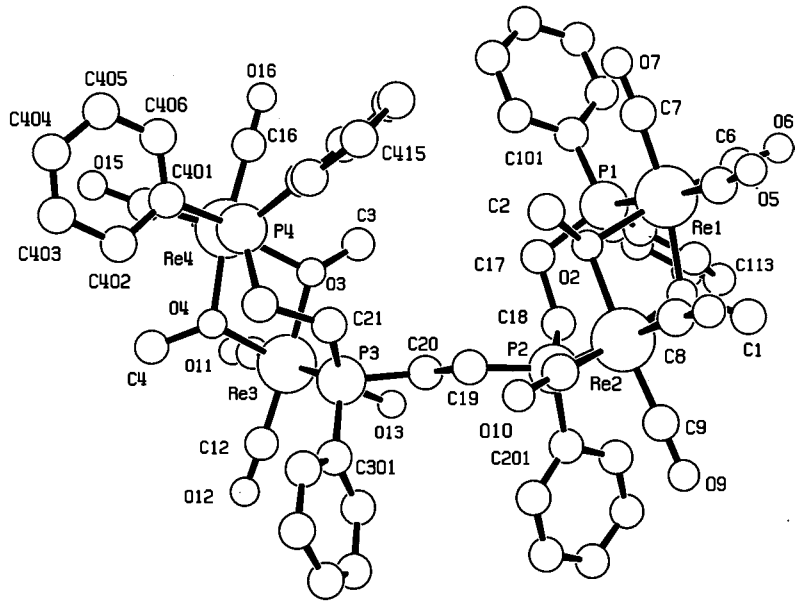

Fig. 2. Crystal structure of *d*/*l*-[{$Re_2(\mu\text{-}OMe)_2(CO)_6$}$_2$($\mu,\mu'$-hptpd)] **1** (hydrogen atoms omitted for clarity).

conformation. The twisting of the CH_2–CH_2 axes most probably results in the interchange of the molecular conformation between {δ[P(1)–P(2)], λ[P(3)–P(4)]} and {λ[P(1)–P(2)], δ[P(3)–P(4)]}. This twisting motion is probably correlated with the rotation of the phenyl rings. The *anti* conformation of the central {PCH_2-CH_2P} segment is probably maintained throughout, since that minimizes the steric interaction between the two bulky {$Re_2(\mu\text{-}OMe)_2(PP)$} fragments.

2.1.4. Raman spectra of meso- and d/l-1

The X-ray crystallographic studies on *d*/*l*- and *meso*-**1** have shown that while the molecules of the former do not possess any symmetry elements, molecules of the latter possess both molecular and crystallographic *i*-symmetry. The solid-state Raman spectrum of *meso*-**1** is thus expected to contain fewer CO stretching peaks than that of the *d*/*l* isomers. The CO stretching absorptions in the IR spectra of both *d*/*l*- and *meso*-**1** are very intense and poorly resolved, resulting in broad ν_{CO} envelopes instead of sharp peaks. The ν_{CO} intensities in the Raman spectra, on the other hand, should be much weaker, and should give well-resolved peaks.

The Raman spectra of *meso*- and *d*/*l*-**1** in the ν_{CO} region are shown in Fig. 5. It is evident that the diastereomers give distinctive spectra and that there are fewer peaks in the spectrum of the *meso* isomer. Raman spectroscopic studies of rhenium carbonyl complexes are uncommon [10]; especially the use of Raman spectroscopy to differentiate diastereomeric carbonyl complexes.

2.2. Reactions of other multidentate phosphines with $Re_2(CO)_{10}$, Me_3NO and MeOH

2.2.1. Tris[2-(diphenylphosphino)ethyl]phosphine (tdppep)

The reaction of the tetraphosphine tdppep with the mixture of $Re_2(CO)_{10}$, Me_3NO and MeOH affords the complex [{$Re_2(\mu\text{-}OMe)_2(CO)_6$}($\mu,\eta^2$-tdppep)] **2** as the main product (21% based on Re). Only two of the phosphorus atoms of the tdppep ligand are coordinated to the {$Re_2(\mu\text{-}OMe)_2(CO)_6$} fragment, the other two remaining free. There is no evidence for the formation of any quadridentate coordinated tdppep-mono-rhenium species that are analogous to the other tdppep complexes reported [11].

It is interesting to note that the {$Re_2(\mu\text{-}OMe)_2$} core is bonded to the central phosphino group and one terminal phosphino group of the ligand, rather than to two terminal phosphino groups, i.e. [Re–$P(CH_2)_2$P–Re] and not [Re–$P(CH_2)_2P(CH_2)_2$P–Re]. This again illustrates the preference of the {$Re_2(\mu\text{-}OMe)_2(CO)_6$} fragment for short-chain diphosphines [3c].

2.2.2. Bis[2-(diphenylphosphino)ethyl]phenylphosphine (triphos)

The reaction of triphos with the mixture of $Re_2(CO)_{10}$, Me_3NO and MeOH affords the complexes [{$Re_2(\mu\text{-}OMe)_2(CO)_6$}($\mu,\mu',\eta^3$-triphos){$Re_2(CO)_9$}] **3** and [{$Re_2(\mu\text{-}OMe)_2(CO)_6$}($\mu,\eta^2$-triphos)] **4**, with yields of 10 and 9%, respectively. As in complexes **1** and **2**, the {$Re_2(\mu\text{-}OMe)_2$} moieties in **3** and **4** are bonded to the [P–CH_2–CH_2–P] fragment of the triphos ligand. Whilst the third phosphino group in **4** is uncoordinated, that in **3** is coordinated to an [$Re_2(CO)_9$] fragment. It can

thus be deduced that $Re_2(CO)_9(L)$ and rhenium methoxo carbonyl species are co-existent in the mixture of $Re_2(CO)_{10}$, Me_3NO and MeOH. No tridentate coordinated mono-rhenium complexes of triphos similar to those reported [12] were isolated from the reaction mixture.

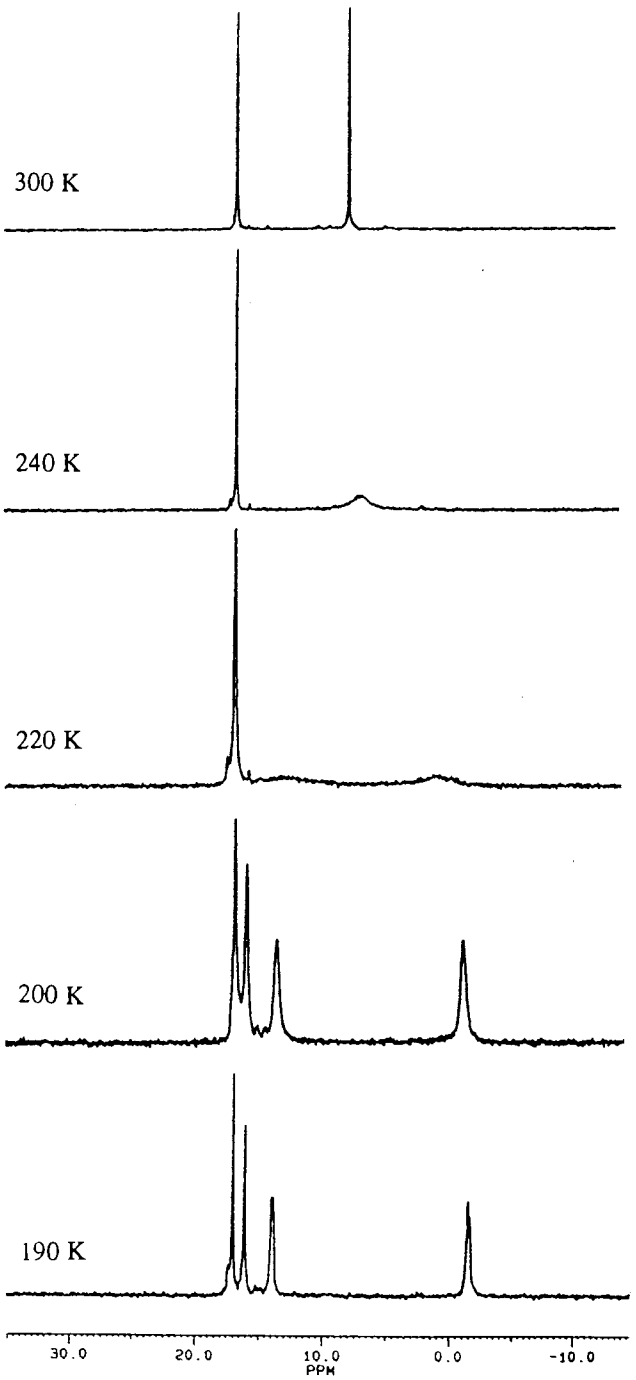

Fig. 3. Variable-temperature ^{31}P-$\{^1H\}$-NMR spectra of *d*/*l*-[$\{Re_2(\mu\text{-}OMe)_2(CO)_6\}_2(\mu,\mu'\text{-hptpd})$] **1** in CD_2Cl_2 (121.5 MHz, 300–190 K).

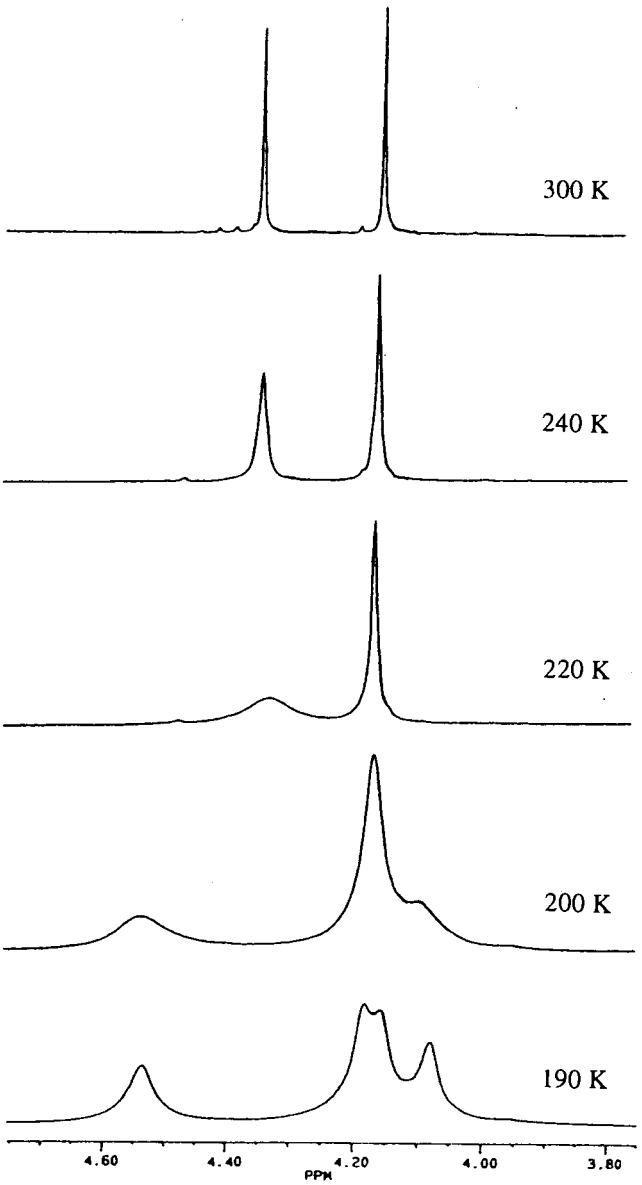

Fig. 4. Variable-temperature ^1H-NMR spectra of *d*/*l*-[$\{Re_2(\mu\text{-}OMe)_2(CO)_6\}_2(\mu,\mu'\text{-hptpd})$] **1** in CD_2Cl_2 (121.5 MHz, 300–190 K).

2.2.3. 1,1,1-Tris(diphenylphosphinomethyl)ethane (tdppme)

The reaction of the triphosphine tdppme with the mixture of $Re_2(CO)_{10}$, Me_3NO and MeOH gave oily products which could not be crystallized, even after isolation by TLC. The major product gave FT-IR and ^{31}P-$\{^1H\}$-NMR spectra that are consistent with the formulation [$Re_2(CO)_9$(tdppme)], with a unidentate-coordinated tdppme ligand. There is no evidence for the formation of species containing the $\{Re_2(\mu\text{-}OMe)_2(CO)_6\}$ fragment or that of tridentate coordinated mono-rhenium–tdppme species analogous to those reported [13].

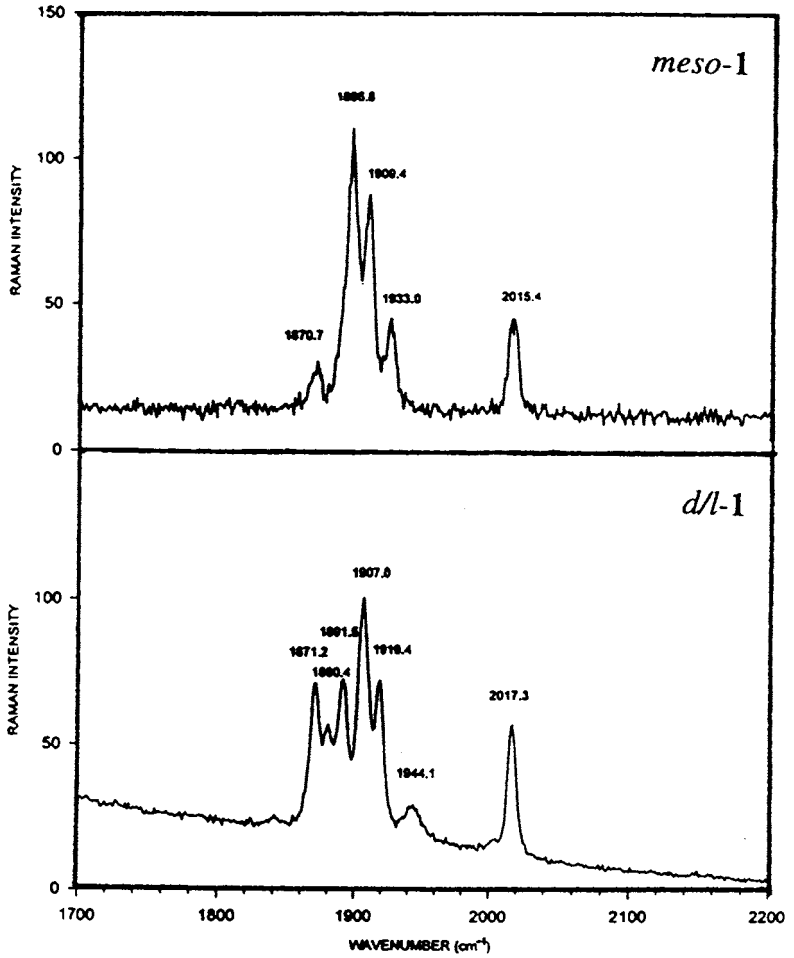

Fig. 5. Solid-state laser Raman spectra of *meso* and *d*/*l*-[{$Re_2(\mu\text{-}OMe)_2(CO)_6$}$_2$($\mu,\mu'$-hptpd)] **1** in the ν_{CO} region.

3. Summary and conclusions

Reactions of the mixture of $Re_2(CO)_{10}$, Me_3NO and MeOH with tetra- and tridentate phosphines afford novel polyphosphine-coordinated rhenium methoxo carbonyl complexes. The tetraphosphine hptpd gives a diastereomeric mixture of *meso*- and *d*/*l*-[{$Re_2(\mu\text{-}OMe)_2(CO)_6$}$_2$($\mu,\mu'$-hptpd)] **1**, which can be easily separated by extraction with benzene. Reactions with the tetraphosphine tdppep and triphosphine triphos yield the complexes [{$Re_2(\mu\text{-}OMe)_2(CO)_6$}($\mu,\eta^2$-tdppep)] **2**, [{$Re_2(\mu\text{-}OMe)_2(CO)_6$}($\mu,\mu',\eta^3$-triphos){$Re_2(CO)_9$}] **3** and [{$Re_2(\mu\text{-}OMe)_2(CO)_6$}($\mu,\eta^2$-triphos)] **4**, respectively. The formation of complexes **1**–**4** confirms the affinity of the {$Re_2(\mu\text{-}OMe)_2(CO)_6$} fragment for a bridging {PCH_2CH_2P} unit, since all the available {PCH_2CH_2P} units in each of the polyphosphines used are bonded to {$Re_2(\mu\text{-}OMe)_2(CO)_6$} fragments. Any remaining phosphino groups not coordinated to {$Re_2(\mu\text{-}OMe)_2(CO)_6$} units are either left uncoordinated or are terminally bonded to {$Re_2(CO)_9$} fragments. The complex *d*/*l*-**1** is fluxional at room temperature; the fluxional motion probably involves the twisting of the two terminal CH_2–CH_2 axes in the hptpd backbone, which is correlated with the rotation of the phenyl rings.

4. Experimental

All reactions were performed under pure dry argon using standard Schlenk techniques. Solvents used were of reagent grade and were dried by published procedures and freshly distilled under argon before use. All other reagents were of AR grade and were obtained from commercial sources unless stated otherwise. All the polyphosphines were purchased from Aldrich and used as supplied. Precoated silica plates of layer thickness 0.25 mm were obtained from Merck. ^{1}H- and ^{31}P-{^{1}H}-NMR spectra were recorded at ca. 300 K at operating frequencies of 300.0 and 121.5 MHz, respectively. ^{1}H and ^{31}P chemical shifts are quoted in ppm downfield of tetramethylsilane and external 80% H_3PO_4, respectively. Infrared spectra were recorded on a Perkin–Elmer 1600 FT-IR Spectrometer or a Bio-Rad

FT-IR Spectrometer. Laser Raman spectra were run using a Renishaw Raman Spectrometer with a 782 nm laser and a scan range of 150–3000 cm^{-1}. The Raman samples in microcrystalline form were loaded on a platinum plate and covered with thin silica glass. Elemental analyses were performed by the Microanalytical Laboratory, Department of Chemistry, National University of Singapore.

4.1. Reaction of the mixture of $Re_2(CO)_{10}$, Me_3NO and MeOH with 1,1,4,7,10,10-hexaphenyl-1,4,7,10,-tetraphosphadecane (hptpd)

A solution of $Me_3NO{\cdot}2H_2O$ (0.062 g, 0.56 mmol) in THF–MeOH(1:1, 20 cm^3) was transferred into a Schlenk flask containing a stirred solution of $Re_2(CO)_{10}$ (0.151 g, 0.23 mmol) in THF(10 cm^3) at room temperature (r.t.). The resultant yellow solution was stirred in vacuo for 4 h at r.t. This intermediate solution was clear green–yellow. Solid $Ph_2P(CH_2)_2P(Ph)(CH_2)_2$-$P(Ph)(CH_2)_2PPh_2$, hptpd (0.077 g, 0.115 mmol) was then introduced and the light-yellow solution so formed was stirred in vacuo for 1 h. The solution was stirred for another 3 h under argon. The solution became colorless and solvent was removed under reduced pressure. The resultant white residue was redissolved in a minimum amount of CH_2Cl_2 and chromatographed on silica TLC plates (2:3 CH_2Cl_2–hexane).

The mixture of *meso*- and *d*/*l*-[{$Re_2(\mu\text{-}OMe)_2(CO)_6$}$_2$($\mu$,$\mu'$-hptpd)] **1** was extracted with CH_2Cl_2 from the main band (R_f 0.23). Layering of the CH_2Cl_2 solution with hexane gave a mixture of *meso*- and *d*/*l*-**1** as a white powder, total yield 0.039 g (18% based on Re). $C_{58}H_{54}O_{16}P_4Re_4$ (f_w 1875.5) requires: C, 37.1; H, 2.9; P, 6.6; Re, 39.7%. Found: C, 37.3; H, 3.0; P, 6.7; Re, 39.7%. The powder was stirred with benzene (20 cm^3) at r.t. for 30 min, during which time *d*/*l*-**1** dissolved. The insoluble *meso*-**1** was separated by filtration and recrystallized by slow evaporation of its solution in CH_2Cl_2–hexane to give colorless prismatic crystals. $\tilde{\nu}_{max}/cm^{-1}$ (CH_2Cl_2) 2026s, 2009m, 1924m, 1899s(sh), 1890s (CO); $\tilde{\nu}_{max}/cm^{-1}$ (THF) 2025s, 2009m, 1924m, 1900s(sh), 1894s (CO). $\delta_P(CD_2Cl_2)$ 15.5(s), 11.3(s); $\delta_H(CD_2Cl_2)$ 7.57–7.18 (m, 30H, Ph), 4.12 (s, 6H, μ-OCH_3), 4.06 (s, 6H, μ-OCH_3), 2.60 (br, 4H, CH_2), 2.11 (br, 4H, CH_2), 1.3 (s, 4H, CH_2).

Colourless plate-like crystals of *d*/*l*-**1** were obtained by layering the benzene solution with hexane. $\tilde{\nu}_{max}/cm^{-1}$ (CH_2Cl_2) 2026s, 2009m, 1924m, 1900s, 1888s (CO); $\tilde{\nu}_{max}/cm^{-1}$ (THF) 2026s, 2009m, 1923m, 1900s(sh), 1880vs (CO); $\tilde{\nu}_{max}/cm^{-1}$ (C_6H_6) 2028s, 2012m, 1927m, 1907s, 1897s 1881s(sh) (CO). $\delta_P(CD_2Cl_2)$ 16.7(s), 7.9(s); δ_H (CD_2Cl_2) 7.57–7.18 (m, 30H, Ph), 4.34 (s, 6H, μ-OCH_3), 4.15 (s, 6H, μ-OCH_3), 2.8 (m, br, 4H, CH_2), 2.2 (br, 4H, CH_2), 1.9 (br, 4H, CH_2). $\delta_P(C_6D_6)$ 16.9(s), 8.4(s); $\delta_H(C_6D_6)$ 7.58–6.93 (m, 30H, Ph), 4.46 (s, 6H, μ-OCH_3), 4.28 (s, 6H, μ-OCH_3), 2.55 (m, br, 4H, CH_2), 2.08 (br, 4H, CH_2), 1.68 (br, 4H, CH_2). Solubility in solvents: CH_2Cl_2, $CHCl_3$ > benzene ≫ hexane. The ratio of yields of *meso* and *d*/*l*-**1** was ca. 3:2.

4.2. Synthesis of meso- and d/l-[{$Re_2(\mu\text{-}OMe)_2(CO)_6$}$_2$-($\mu$,$\mu'$-hptpd)] **1** via controlled acidolysis of [Re_2-$(\mu\text{-}OMe)_3(CO)_6$]$^-$ in the presence of hptpd

A solution of *p*-toluenesulfonic acid monohydrate (0.038 g, 0.20 mmol) in 10 cm^3 of $CHCl_3$ and 10 cm^3 MeOH was transferred into a stirred solution of [Et_4N][$Re_2(\mu\text{-}OMe)_3(CO)_6$] (0.152 g, 0.20 mmol) and hptpd (0.067 g, 0.10 mmol) in 10 cm^3 of $CHCl_3$. The resultant mixture was stirred under argon for 2 h. The solvent was then removed under reduced pressure. The residue obtained was redissolved in a minimum amount of CH_2Cl_2 and chromatographed on silica TLC plates (2:3 CH_2Cl_2–hexane). The mixture of complexes *meso*- and *d*/*l*-[{$Re_2(\mu\text{-}OMe)_2(CO)_6$}$_2$($\mu$,$\mu'$-hptpd)] **1** was isolated from the main band (R_f 0.23) and resolved as described above. Yield of *meso*-**1**, 0.028 g (15%). Yield of *d*/*l*-**1**, 0.048 g (26%).

4.3. Reaction of the mixture of $Re_2(CO)_{10}$, Me_3NO and MeOH with tris[2-(diphenylphosphino)-ethyl]phosphine (tdppep)

The reaction was carried out in a similar manner to that described above except that hptpd was replaced by $(Ph_2PCH_2CH_2)_3P$, tdppep (0.077 g, 0.115 mmol). The residue obtained after evaporation of the reaction mixture was redissolved in a minimum amount of CH_2Cl_2 for TLC (2:3 CH_2Cl_2–hexane). The complex [{$Re_2(\mu\text{-}OMe)_2(CO)_6$}($\mu$,$\eta^2$-tdppep)] **2** was isolated from main band at $R_f = 0.35$, and fine colorless crystals of **3** were obtained from CH_2Cl_2–hexane. Yield 0.064 g (21%). $C_{50}H_{48}O_8P_4Re_2$ (f_w 1273) requires C, 47.1; H, 3.8; P, 9.7%. Found C, 46.6; H, 3.9; P, 9.9%. $\tilde{\nu}_{max}/cm^{-1}$ (CH_2Cl_2) 2024s, 2007m, 1921m, 1896s(sh), 1889vs (CO); $\tilde{\nu}_{max}/cm^{-1}$ ($CHCl_3$) 2025s, 2008m, 1922m, 1897s(sh), 1890vs (CO). $\delta_P(CDCl_3)$: 15.6 (s, 1P, coord. PPh_2), 10.8 (t, 1P, $P(CH_2)_3$, $J_{P-P} = 30$ Hz), −12.6 (d, 2P, uncoord. PPh_2, $J_{P-P} = 30$ Hz); $\delta_H(CDCl_3)$: 7.5–7.3 (m, 30H, Ph), 4.08 (s, 6H, μ-OCH_3), 2.44–2.39 (m, 2H, CH_2), 2.0–1.9 (m, 8H, CH_2), 1.8–1.7 (m, 2H, CH_2).

4.4. Reaction of the mixture of $Re_2(CO)_{10}$, Me_3NO and MeOH with bis(2-diphenylphosphinoethyl)-phenylphosphine (triphos)

The reaction was carried out as described for the reaction with hptpd except that hptpd was replaced by $PhP[CH_2CH_2PPh_2]_2$, triphos (0.082 g, 0.154 mmol). The resultant residue was treated similarly by TLC (2:3

CH_2Cl_2–hexane). The complexes [{$Re_2(\mu\text{-}OMe)_2(CO)_6$}($\mu,\mu',\eta^3$-triphos){$Re_2(CO)_9$}] **3** and [{$Re_2(\mu\text{-}OMe)_2(CO)_6$}($\mu,\eta^2$-triphos)] **4** were isolated from main bands at $R_f = 0.47$ and 0.40, respectively.

Fine off-white crystals of complex **3** were obtained by the slow evaporation of a CH_2Cl_2–hexane solution of the complex over 1 week. Yield 0.021 g (10% based on Re). $C_{51}H_{39}O_{17}P_3Re_4$ (f_w 1761) requires C, 34.8; H, 2.2; P, 5.3%. Found C, 34.1; H, 2.3; P, 5.4%. $\tilde{\nu}_{max}/cm^{-1}$ (CH_2Cl_2) 2106w, 2033w(sh), 2026m, 2007m(sh), 1996vs, 1963m, 1937m(sh), 1925s, 1897s(sh), 1890s (CO) (underlined absorption maxima are assigned to the [$Re_2(\mu\text{-}OMe)_2(CO)_6$] fragment, the others are assigned to the [$Re_2(CO)_9$] fragment). $\delta_P(CD_2Cl_2)$: 16.3 (d, Ph_2P-ReOMe, $J_{P-P} = 6.5$ Hz), 9.6 (dd, PPh–ReOMe, $J_{P-P} = 27$ Hz, $J'_{P-P} = 6.5$ Hz), 8.4 [d, PPh_2–$Re_2(CO)_9$, $J_{P-P} = 27$ Hz]. δ_H (CD_2Cl_2): 7.71–6.90 (m, 25H, Ph), 4.14(s, 3H, μ-OCH_3), 4.06 (s, 3H, μ-OCH_3), 2.8–2.2 (m, br, 8H, CH_2).

Complex **4** was obtained as a white powder by the slow evaporation of a CH_2Cl_2–hexane solution of the complex over 1 week. Yield 0.023 g (9% based on Re). $C_{42}H_{39}O_8P_3Re_2$ (f_w 1137) requires C, 44.3; H, 3.4; P, 8.2%. Found. C, 43.8; H, 3.5; P, 8.1%. $\tilde{\nu}_{max}/cm^{-1}$ (CH_2Cl_2) 2024s, 2008m, 1922m, 1897s(sh), 1890vs (CO). $\delta_H(CD_2Cl_2)$ 7.6–7.2 (m, 25H, Ph), 4.17 (s, 3H, μ-OCH_3), 4.09 (s, 3H, μ-OCH_3), 2.7–1.8 (m, 8H, CH_2); $\delta_P(CD_2Cl_2)$: 15.7 (d, coord. Ph_2P, $J_{P-P} = 6$ Hz), 10.8 (dd, coord. PhP, $J_{P-P} = 29$ Hz, $J'_{P-P} = 6$ Hz), −12.9 (d, free Ph_2P, $J_{P-P} = 29$ Hz).

4.5. Reaction of the mixture of $Re_2(CO)_{10}$, Me_3NO and MeOH with 1,1,1-tris(diphenyl-phosphinomethyl)-ethane (tdppme)

The reaction was carried out as described for the reaction with hptpd except that hptpd was replaced by $CH_3C[CH_2PPh_2]_3$, tdppme (0.096 g, 0.154 mmol). The resultant residue was treated similarly by TLC (2:3 CH_2Cl_2–hexane). The product extracted by CH_2Cl_2 from the main band (R_f 0.73) was oily and could not be crystallized. From its FT-IR and ^{31}P-NMR spectra, the product was tentatively identified as [$Re_2(CO)_9$-(tdppme)]. $\tilde{\nu}_{max}/cm^{-1}$ (CH_2Cl_2) 2103w, 2032w, 1993vs, 1960m, 1933m (CO). $\delta_P(CD_2Cl_2)$: −4.6 (s, 1P, coord. Ph_2P), −7.1 (s, 2P, free Ph_2P).

4.6. X-ray crystallography

The crystallographic data for *meso*- and *d*/*l*-**1** are summarized in Table 1, and selected bond lengths and angles for *meso*-**1** are given in Table 2.

4.6.1. meso-[{$Re_2(\mu\text{-}OMe)_2(CO)_6$}$_2(\mu,\mu'$-hptpd)] **1**

Single colorless crystals of *meso*-**1** were grown by slow evaporation of a solution of the complex in CH_2Cl_2–hexane at r.t. The number of data used for structure solution and refinement was 3807 [$I > 2.0\sigma(I)$]. The structure was solved by direct methods (MULTAN [14]). Refinement (on F) was carried out by the full-matrix least-squares method with all non-hydrogen atoms being allowed anisotropic motion. All hydrogen atoms were held fixed in the final cycles of least-squares refinement. The last least-squares cycle was calculated with 370 parameters and 3807 reflections. The weighting function used was $w^{-1} = \sigma^2(F_o) + 0.000100F_o^2$. The maximum shift/$\sigma$ ratio was less than 0.001. In the last difference map the deepest hole was −0.760 e Å^{-3}, and the highest peak was 0.550 e Å^{-3}. Computations were carried out on a Microvax 3600 computer with the NRCVAX system [15].

Table 1
Crystallographic data for *meso* and *d*/*l*-[{$Re_2(\mu\text{-}OMe)_2(CO)_6$}$_2(\mu,\mu'$-hptpd)] **1** [a]

	meso-**1**	*d*/*l*-**1**
Crystal system	Monoclinic	Triclinic
Space group	$P2_1/n$	$P\bar{1}$
Unit cell dimensions		
a (Å)	13.001(1)	12.963(8)
b (Å)	18.990(2)	13.994(12)
c (Å)	13.267(3)	20.09(2)
α (°)	90	79.32(6)
β (°)	94.76(1)	75.06(5)
γ (°)	90	68.34(5)
V (Å^3)	3264.1(9)	3256(5)
μ (mm^{-1})	7.65	7.57
Absorption corrections	ψ-scans	Face-indexed numerical
Min/max transmission	0.687, 0.999	0.488, 0.736
Diffractometer	Nonius	Siemens P4
Max. 2θ (°)	49.8	50.0
hkl range	−15 to 15, 0 to 22, 0 to 15	−1 to 15, −15 to 16, −23 to 23
Reflections measured	6009	13120
Unique reflections (R_{int})	5742 (0.015, based on F)	11460 (0.061, based on F^2)
R_1, [b] wR [c] [$I > 2\sigma(I)$]	0.028, 0.029 (R_w) [d]	0.070, 0.135

[a] Details in common: chemical formula $C_{58}H_{54}O_{16}P_4Re_4$; M, 1875.7; Z, 2; temperature of 297 ± 2 K; graphite-monochromated Mo–K_α radiation; $\theta - 2\theta$ scan mode.
[b] $R_1 = \Sigma \| |F_o| - |F_c| \| / \Sigma |F_o|$.
[c] $wR = [\Sigma w(F_o^2 - F_c^2)^2 / \Sigma w(F_o^2)^2]^{1/2}$.
[d] $R_w = [\Sigma w(|F_o| - |F_c|)^2 / \Sigma w|F_o|^2]^{1/2}$.

4.6.2. d/l-[{$Re_2(\mu\text{-}OMe)_2(CO)_6$}$_2(\mu,\mu'$-hptpd)] **1**

Single colorless crystals of *d*/*l*-**1** were grown by layering a solution of the compound in benzene with hexane. The number of data used for structure solution and refinement was 5980 [$I > 2.0\sigma(I)$]. The structure was solved by the heavy-atom method. All non-hydrogen atoms were refined anisotropically by the full-matrix

Table 2
Selected bond lengths (Å) and angles (°) for complex *meso*-[{Re_2-(μ-OMe)$_2$(CO)$_6$}$_2$(μ,μ′-hptpd)] **1**

Bond lengths			
Re(1)···Re(2)	3.3966(9)	Re(1)–P(1)	2.485(2)
Re(1)–C(1)	1.889(9)	Re(1)–C(2)	1.939(10)
Re(1)–C(3)	1.894(10)	Re(1)–O(7)	2.146(5)
Re(1)–O(8)	2.140(5)	Re(2)–P(2)	2.478(2)
Re(2)–C(4)	1.916(10)	Re(2)–C(5)	1.932(9)
Re(2)–C(6)	1.896(9)	Re(2)–O(7)	2.161(5)
Re(2)–O(8)	2.148(5)		
Bond angles			
P(1)–Re(1)–C(1)	88.5(3)	P(1)–Re(1)–C(2)	174.5(3)
P(1)–Re(1)–C(3)	93.7(3)	P(1)–Re(1)–O(7)	90.1(1)
P(1)–Re(1)–O(8)	83.7(1)	O(7)–Re(1)–O(8)	73.3(2)
O(7)–Re(1)–C(3)	97.8(3)	O(8)–Re(1)–C(3)	170.7(3)
C(1)–Re(1)–C(3)	87.5(4)	P(2)–Re(2)–C(4)	90.8(3)
P(2)–Re(2)–C(5)	174.7(2)	P(2)–Re(2)–C(6)	88.4(3)
P(2)–Re(2)–O(7)	89.0(1)	P(2)–Re(2)–O(8)	86.2(1)
O(7)–Re(2)–O(8)	72.8(2)	O(7)–Re(2)–C(5)	95.5(3)
O(8)–Re(2)–C(5)	97.8(3)	C(4)–Re(2)–C(6)	87.5(4)
Re(1)–O(7)–Re(2)	104.2(2)	Re(1)–O(8)–Re(2)	104.8(2)
Re(1)–P(1)–C(9)	120.4(2)	Re(2)–P(2)–C(10)	116.9(2)
P(1)–C(9)–C(10)	115.6(5)	P(2)–C(10)–C(9)	113.8(5)

least-squares method (on F^2). Hydrogen atoms were introduced in calculated positions and refined isotropically (riding model) in the final cycles of least-squares refinement. The last least-squares cycle was calculated with 721 parameters and 11 401 data (all of the unique reflections except very negative ones). The weighting function used was $w^{-1} = \sigma^2(F_o^2) + (0.0600P)^2$, where $P = (F_o^2 + 2F_c^2)/3$. The maximum shift/σ ratio was 0.008. In the last difference map the deepest hole was -2.467 e Å^{-3}, and the highest peak was 2.352 e Å^{-3} [within 1 Å from Re(2)]. Computations were carried out on a Pentium PC using the SHELXTL PLUS software package [16].

5. Crystallographic data

Crystallographic data for the structural analysis has been deposited with the Cambridge Crystallographic Data Centre, CCDC nos. 127345 for *meso*-**1**, 121769 for *d*/*l*-**1**.

Acknowledgements

We thank the National University of Singapore (NUS) (RP 950695), the National Institute of Education, Nanyang Technological University (RP 15/95 YYK), and the Academia Sinica, Taipei, for financial support. Technical assistance from the staff of the NMR Laboratory, Department of Chemistry, NUS is acknowledged. C.H.J. is grateful to NUS for a scholarship award.

References

[1] (a) S.K. Mandal, D.M. Ho, M. Orchin, Organometallics 12 (1993) 1714. (b) R.G. Bergman, Polyhedron 14 (1995) 3227. (c) R.D. Simpson, R.G. Bergman, Organometallics 12 (1993) 781. (d) R.D. Simpson, R.G. Bergman, Organometallics 11 (1992) 4306.

[2] (a) H.E. Bryndza, W. Tam, Chem. Rev. 88 (1988) 1163. (b) J.D. Gargulak, A.J. Berry, M.D. Noirot, W.L. Gladfelter, J. Am. Chem. Soc. 114 (1992) 8933. (c) D.J. Darensbourg, B.L. Mueller, J.H. Reibenspies, C.J, Bischoff, Inorg. Chem. 29 (1990) 1789.

[3] (a) C.H. Jiang, Y.-S. Wen, L.-K. Liu, T.S.A. Hor, Y.K. Yan, Organometallics 17 (1998) 173. (b) C.H. Jiang, Y.-S. Wen, L.-K. Liu, T.S.A. Hor, Y.K. Yan, J. Organomet. Chem. 543 (1997) 179. (c) P.M.N. Low, Y.L. Yong, Y.K. Yan, T.S.A. Hor, S.-L. Lam, K.K. Chan, C. Wu, S.C.F. Au-Yeung, Y.-S. Wen, L.-K. Liu, Organometallics 15 (1996) 1369. (d) Y.K. Yan, H.S.O. Chan, T.S.A. Hor, K.L. Tan, L.-K. Liu, Y.-S. Wen, J. Chem. Soc. Dalton Trans. (1992) 423. (e) T.S.A. Hor, C.F. Lam, Y.K. Yan, Bull. Singap. Natl. Inst. Chem. 19 (1991) 115. (f) S.L. Lam, Y.X. Cui, S.C.F. Au-Yeung, Y.K. Yan, T.S.A. Hor, Inorg. Chem. 33 (1994) 2407.

[4] (a) R.B. King, P.N. Kapoor, J. Am. Chem. Soc. 91 (1969) 5191. (b) R.B. King, P.N. Kapoor, J. Am. Chem. Soc. 93 (1971) 4158.

[5] (a) H.A. Mayer, W.C. Kaska, Chem. Rev. 94 (1994) 1239. (b) R.B. King, J.C. Cloyd, Jr., Inorg. Chem. 14 (1975) 1550. (c) R.B. King, P.N. Kapoor, Inorg. Chem. 11 (1972) 1524.

[6] (a) A.L. Airey, G.F. Swiegers, A.C. Willis, S.B. Wild, Inorg. Chem. 36 (1997) 1588. (b) C. Bachmann, W. Oberhauser, P. Brueggeller, Polyhedron 15 (1996) 2223. (c) K. Dillinger, W. Oberhauser, Ch. Bachmann, P. Brueggeller, Inorg. Chim. Acta 223 (1994) 13. (d) H. Goller, P. Brueggeller, Inorg. Chim. Acta 197 (1992) 75. (e) W. Oberhauser, Ch. Bachmann, P. Brueggeller, Polyhedron 14 (1995) 787. (f) J.-D. Chen, F.A. Cotton, B. Hong, Inorg. Chem. 32 (1993) 2343. (g) R. Cotton, J.C. Traeger, V. Tedesco, Inorg. Chim. Acta 210 (1993) 193.

[7] (a) F.A. Cotton, B. Hong, M. Shang, G.G. Stanley, Inorg. Chem. 32 (1993) 3620. (b) D.E. Rende, Y. Kim, C.M. Beck, A. Wojcicki, Inorg. Chim. Acta 240 (1995) 435.

[8] J.N. Brown, L.R. Canning, J. Organomet. Chem. 267 (1984) 179.

[9] A.L. Airey, G.F. Swiegers, A.C. Willis, S.B. Wild, Inorg. Chem. 36 (1997) 1588.

[10] U.A. Jayasoorya, C.E. Anson, O. Al-Jowder, G. D'Alfonso, P.L. Stanghellini, R. Rossetti, Surf. Sci. 294 (1993) 131.

[11] D.M. Heinekey, M. van Roon, J. Am. Chem. Soc. 118 (1996) 12134.

[12] (a) Y. Kim, FJ. Gallucci, A. Wojcicki, Organometallics 11 (1992) 1963. (b) Y. Kim, H. Deng, D.W. Meek, A. Wojcicki, J. Am. Chem. Soc. 112 (1990) 2798. (c) X.-L. Luo, R.H. Crabtree, J. Chem. Soc. Dalton Trans. (1991) 587. (d) Y. Kim, J. Gallucci, A. Wojcicki, J. Am. Chem. Soc. 112 (1990) 8600.

[13] (a) S.P. Ginsberg, S.C. Abrahams, P. Marsh, K. Ataka, C.R.F. Sjprinkle, J. Chem. Soc. Chem. Commun. (1984) 1321. (b) S.C. Abrahams, A.P. Ginsberg, T.F. Koetzle, P. Marsh, C.P. Sprinkle, Inorg. Chem. 25 (1986) 2500. (c) M.T. Costello, P.E. Fanwick, M.A. Green, R.A. Walton, Inorg. Chem. 31 (1992) 2359. (d) H.P. Guntz, G.J. Leigh, J. Chem. Soc. A (1971) 2229. (e) J. Ellermann, H.A. Lindner, M. Moll, Chem. Ber. 112 (1979) 3441. (f) J. Ellermann, H.A. Lindner, H. Gaebelein, J. Organomet. Chem. 172 (1979) 39. (g) C. Bianchini, M. Peruzzini, F. Zanobini, L. Magon, L. Marvellik, R. Rossi, J. Organomet. Chem. 451 (1993) 97.

[14] P. Main, S.E. Fiske, S.L. Hull, G. Germaine, J.P. Declerq, M.H. Woolfson, MULTAN, A System of Computer Programs for Crystal Structure Determination from X-ray Diffraction Data, University of York and Louvain, Belgium, 1980.
[15] E.J. Gabe, Y. Le Page, J.-P. Charland, F.L. Lee, P.S. White, J. Appl. Cryst. 22 (1989) 384.
[16] G.M. Sheldrick, SHELXTL PC, Version 5.03, Siemens Analytical X-ray Instruments Inc., Madison, WI, 1994.